Journal of Ceramic Processing Research. Vol. 17, No. 3, pp. 156~160 (2016)

J O U R N A L O F
Ceramic Processing Research

Properties and rapid consolidation of (W,Ti)C-CNT by pulsed current activated sintering

Seung-Jin Oh[a], Byung-Su Kim[b] Jin-Kook Yoon[c] and In-Jin Shon[a,*]

[a]*Division of Advanced Materials Engineering and the Research Center of Advanced Materials Development, Engineering College, Chonbuk National University, 561-756, Korea*

[b]*Minerals Resources Research Division, Korea Institute of Geoscience and Mineral Resources, Daejeon 305-350, Korea*

[c]*Materials Architecturing Research Center, Korea Institute of Science and Technology, P.O. Box 131, Cheongryang, Seoul 130-650, Korea*

The grain size of (W,Ti)C powder remarkably decreases with a high-energy ball milling. The rapid sintering of nanostuctured (W,Ti)C and (W,Ti)C-CNT hard materials was investigated with pulsed current activated sintering. The advantage of this process is that it allows very quick densification to near theoretical density and prohibition of grain growth in nanostuctured materials. A dense nanostructured (W,Ti)C and (W,Ti)C-CNT hard material with a relative density of up to 99% was produced with simultaneous application of 80 MPa pressure and a pulsed current of 2000A within 3 minutes. The effect of CNT on the sintering behavior and mechanical properties of (W,Ti)C was investigated.

Key words: Nanomaterials, Sintering, Hardness, Fracture Toughness, Hard Materials

Introduction

(W,Ti)C has a high melting point and high hardness. In this regard, the transition metal carbide is primarily used as cutting tools and abrasive materials as a single phase or composite structures. In the case of cemented (W,Ti)C, Co or Ni is added as a binder for the formation of composite structures. However, the high cost of Co or Ni and the low corrosion resistance of the (W,Ti)C-Co or (W,Ti)C-Ni cermet have generated interest in recent years to find alternative binder phases [1-4]. It has been reported that CNT shows a high hardness, elastic modulus, strength, good resistance to corrosion and cheaper material when compared to Co and Ni [5].

Nanocrystalline materials have received much attention as advanced engineering materials with improved physical and mechanical properties. Since nanomaterials possess high strength, high hardness, excellent ductility and toughness, undoubtedly, more attention has been paid to the application of nanomaterials [6-8]. In recent days, nanocrystalline powders have been developed by the thermochemical and thermomechanical process named the spray conversion process (SCP), co-precipitation and high energy milling [9-11]. However, the grain size in sintered materials becomes much larger than that in pre-sintered powders due to the rapid grain growth during a conventional sintering process. Therefore, although the initial particle size is less than 100 nm, the grain size increases rapidly up to 500 nm or larger during conventional sintering [12]. So, controlling grain growth during sintering is one of the keys to the commercial success of nanostructured materials. In this regard, pulsed current activated sintering (PCAS) which can make dense materials within 2 minutes has been shown to be effective in achieving this goal [13-15].

In this study, we investigated the effect of CNT on sintering behavior and mechanical properties of the (W,Ti)C by the PCAS method. The goal of this research is to produce nanopowder and dense nanostructured (W,Ti)C-CNT composites.

Experimental Procedures

The (W,Ti)C powder with a grain size of < 1 mm and 99% purity and CNT used in this research was supplied by H.C. Starck and Carbon Nanotechnology Inc. respectively. The powders were first milled in a high-energy ball mill (Pulverisette-5 planetary mill) at 250 rpm for 10 h. Tungsten carbide balls (9 mm in diameter) were used in a sealed cylindrical stainless steel vial under an argon atmosphere. The weight ratio of balls-to-powder was 30 : 1. Milling resulted in a significant reduction in grain size. The grain size of the (W,Ti)C was calculated from the full width at half-maximum (FWHM) of the diffraction peak by Suryanarayana and Grant Norton's formula [16].

$$B_r\ (B_{crystalline} + B_{strain})\ \cos\theta = k\ \lambda\ /\ L + \eta \sin\theta \qquad (1)$$

where B_r is the full width at half-maximum (FWHM)

*Corresponding author:
Tel : +82-63-270-2381
Fax: +82-63-270-2386
E-mail: ijshon@chonbuk.ac.kr

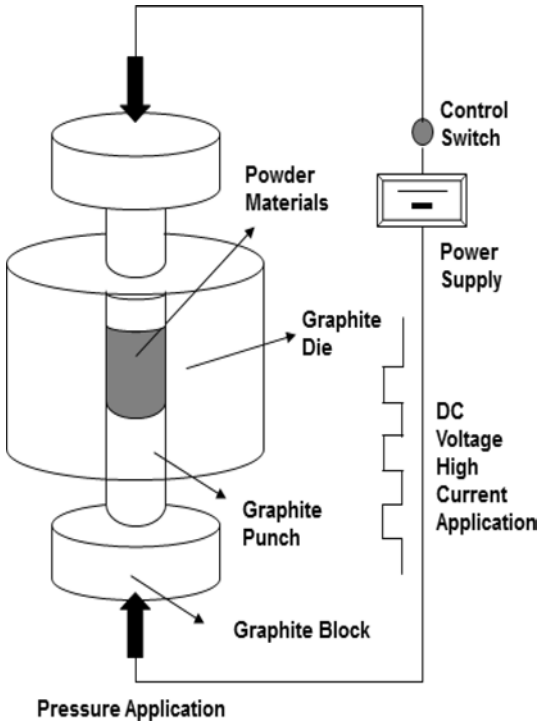

Fig. 1. Schematic diagram of the apparatus for pulsed current activated sintering.

of the diffraction peak after instrumental correction; $B_{crystalline}$ and B_{strain} are the FWHM caused by the small grain size and internal stress, respectively; k is a constant (with a value of 0.9); λ is the wavelength of the X-ray radiation; L and η are the grain size and internal strain, respectively; and θ is the Bragg angle. The parameters B and B_r follow Cauchy's form with the relationship: $B = B_r + B_s$, where B and B_s are the FWHM of the broadened Bragg peaks and the standard sample's Bragg peaks, respectively.

The powders were placed in a graphite die (outside diameter, 35 mm; inside diameter, 10 mm; height, 40 mm) and then introduced into the pulsed current activated sintering (PCAS) apparatus shown schematically in Fig. 1. The PCAS apparatus includes a 30 kW power supply which provides a pulsed current (on time; 20 μs, off time; 10 μs) through the sample, and a 50 kN uniaxial load. The system was first evacuated and a uniaxial pressure of 80 MPa was applied. A pulsed current was then activated and maintained until the densification rate was negligible, as indicated by the real-time output of the shrinkage of the sample. The shrinkage was measured by a linear gauge measuring the vertical displacement. Temperatures were measured by a pyrometer focused on the surface of the graphite die. At the end of the process, the induced current was turned off and the sample cooled to room temperature. The process was carried out under a vacuum of 4×10^{-2} Torr (5.33 Pa).

The relative density of the sintered sample was measured by the Archimedes method. Microstructural information was obtained from product samples, which had been polished and etched using Murakami's reagent (10 g potassium ferricyanide, 10 g NaOH, and 100 ml water) for 1-2 minutes at room temperature. Compositional and microstructural analyses of the products were made through X-ray diffraction (XRD), scanning electron microscopy (SEM) with energy dispersive X-ray spectroscopy (EDS) and a field emission scanning electron microscope (FE-SEM). Vickers hardness was measured by performing indentations at a load of 10 kg_f and a dwell time of 15 s.

Results and Discussion

Fig. 2 shows FE-SEM images of the (W,Ti)C, (W,Ti)C-5 vol.% CNT and (W,Ti)C-10 vol.% CNT powders after milling for 10 h. (W,Ti)C powder has a nano-size, round shape and some agglomeration. EDS of (W,Ti)C-10 vol.% CNT powder milled for 10 h is shown in Fig. 3. In EDS W, Ti and C peaks are detected. The milling process is known to introduce impurities from the ball and/or container. However, in this study, peaks of Fe was not identified.

The variations of the shrinkage displacement and

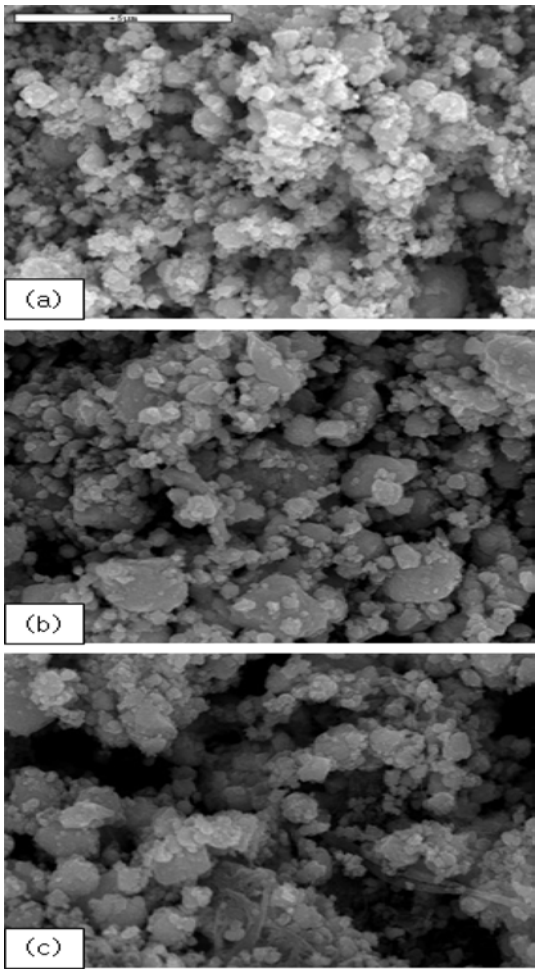

Fig. 2. FE-SEM images of (a) (W,Ti)C, (b) (W,Ti)C-5 vol.%CNT and (c) (W,Ti)C-10 vol.%CNT powder after milling for 10 h.

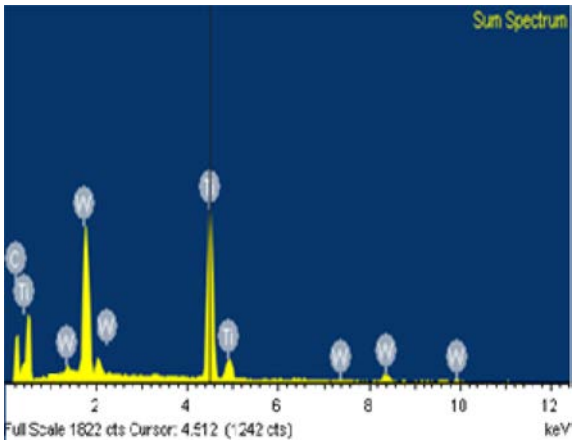

Fig. 3. EDS of the (W,Ti)C-10 vol.%CNT powders with milling for 10 h.

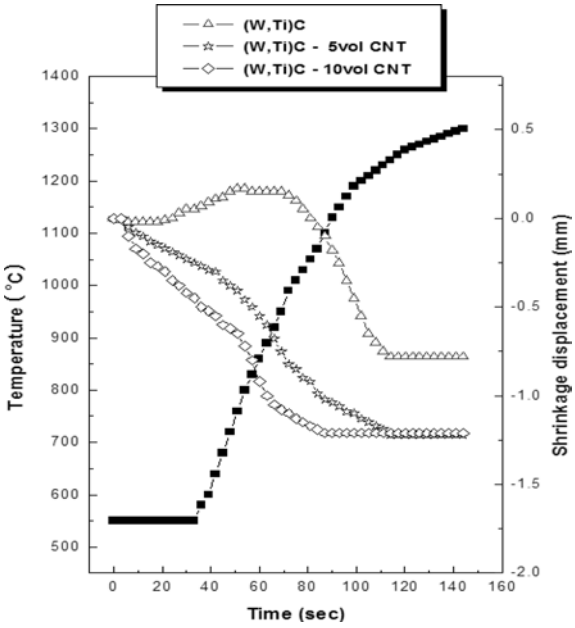

Fig. 4. Variations of temperature and shrinkage with heating time during the pulsed current activated sintering of (W,Ti)C, (W,Ti)C-5 vol.%CNT and (W,Ti)C-10 vol.%CNT powders milled for 10 h.

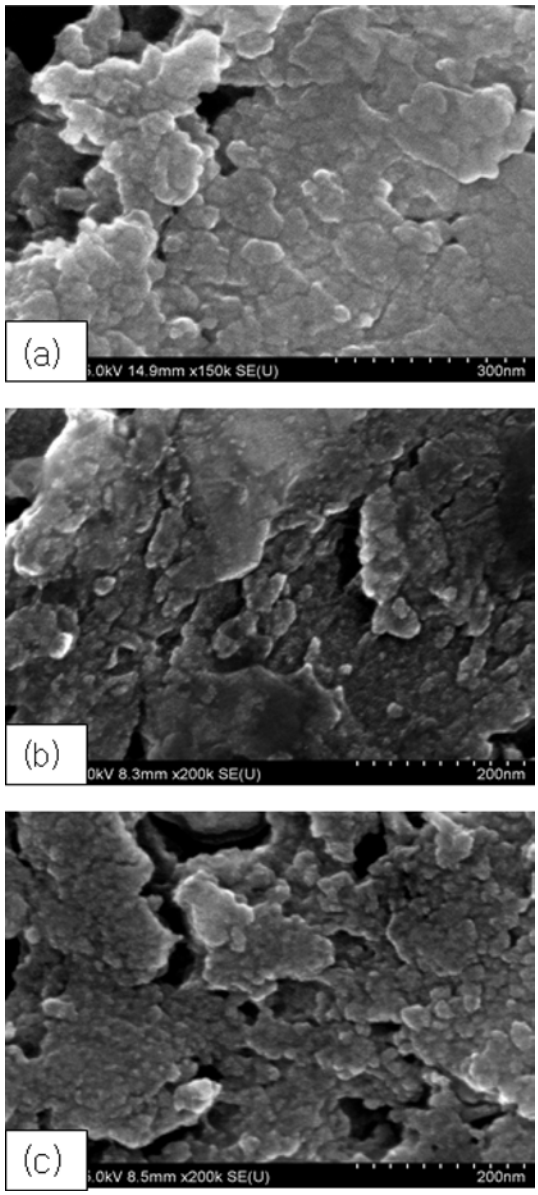

Fig. 5. FE-SEM images of (a) (W,Ti)C, (b) (W,Ti)C-5 vol.%CNT and (c) (W,Ti)C-10 vol.%CNT sintered from powders after milling for 10 h.

temperature with the heating time for a pulsed current 2000A during the sintering of the high energy ball milled (W,Ti)C, (W,Ti)C-5 vol.% CNT and (W,Ti)C-10 vol.% CNT powders under a pressure of 80 MPa are shown in Fig. 4. In all cases, the application of the pulsed current resulted in shrinkage due to consolidation. In case of (W,Ti)C, the thermal expansion shows as soon as a pulsed current is applied. However, in the case of (W,Ti)C-5 vol.% CNT and (W,Ti)C-10vol.% CNT powders, the shrinkage continuously increases up to 1300 °C. The temperature at which shrinkage started decreased with increasing CNT content. It is considered that CNT affected the rate of densification because atomic diffusion increases with addition of CNT [17]. Fig. 5 shows FE-SEM images of (W,Ti)C, (W,Ti)C-5 vol.% CNT and (W,Ti)C-10 vol.% CNT sintered from the 10h milled powders. From the figures, it is known that the (W,Ti)C is consisted of nanoparticle. And their corresponding relative density is about 99%. The use of spark plasma sintering (SPS) to successfully consolidate WC powders (without a binder) has been demonstrated in several investigations. An example of this is a recent work in which unmilled 40-70 nm WC powders were consolidated at 1500 °C to a relative density of up to 95.5% under a pressure of 126 MPa and a current of 3000 A [18]. Comparing the above study with ours, the sintering temperature of the high energy mechanical milled (W,Ti)C is lower than that of the unmilled powder, due to the increase in the reactivity of the powder, the internal and surface energy as well as the surface area, which all contribute

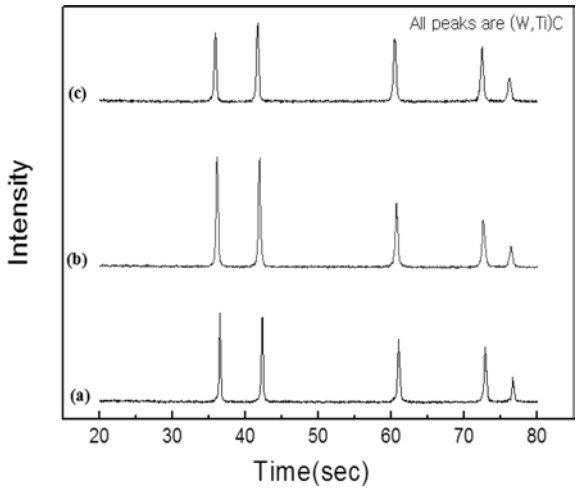

Fig. 6. XRD patterns of (a) (W,Ti)C, (b) (W,Ti)C-5 vol.%CNT and (c) (W,Ti)C-10 vol.%CNT sintered from powders after milling for 10 h.

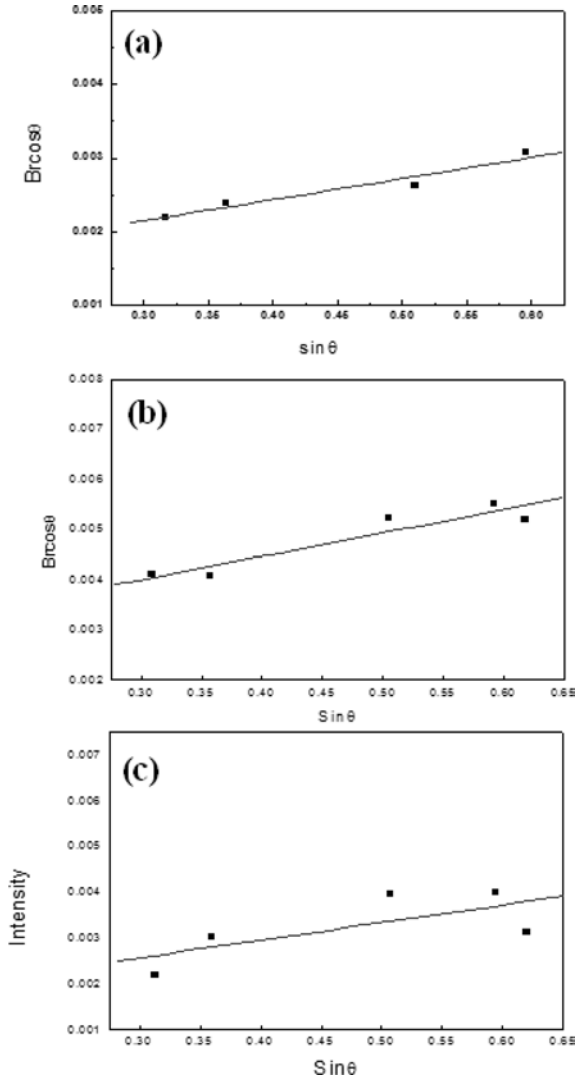

Fig. 7. Plots of B_r ($B_{crystallite} + B_{strain}$) cosè versus sinè for (W,Ti)C in (a) (W,Ti)C-0vol%CNT, (b) (W,Ti)C-5 vol.%CNT and (c) (W,Ti)C-10vol.%CNT sintered from powders after milling for 10 h.

to its so-called mechanical activation [19]. Fig. 6 shows the XRD patterns of the (W,Ti)C, (W,Ti)C-5 vol.% CNT and (W,Ti)C-10 vol.% CNT sintered for milled powders used in this study. All peaks are from (W,Ti)C. Plots of B_r ($B_{crystalline} + B_{strain}$) cosè versus sinè in Suryanarayana and Grant Norton's formula [16] are shown in Fig. 7. The average grain sizes of the (W,Ti)C in 0 vol.% CNT, 5 vol.% CNT and 10 vol.% CNT calculated from the XRD data were about 60, 52, and 66 nm, respectively. Thus, the average grain size of the sintered (W,Ti)C is not greatly larger than that of the initial powder, indicating the absence of much grain growth during sintering. This retention of the grain size is attributed to the high heating rate and the relatively short term exposure of the powders to the high temperature.

The role of the current (resistive or inductive) in sintering has been the focus of several attempts aimed at providing an explanation of the observed enhancement of sintering and the improved characteristics of the products. The role played by the current has been variously interpreted, the effect being explained in terms of a fast heating rate due to Joule heating, the presence of a plasma in pores separating powder particles, and the intrinsic contribution of the current to rapid mass transport [20-23].

Vickers hardness measurements were performed on polished sections of the (W,Ti)C, (W,Ti)C-5 vol.% CNT and (W,Ti)C-10 vol.% CNT samples using a 10 kg_f load and 15 s dwell time. Indentations with large enough loads produced radial cracks emanating from the corners of the indent. The lengths of these cracks permit estimation of the fracture toughness of the materials by means of the expression [24]:

$$K_{IC} = 0.203(c / a)^{-3/2} \cdot H_v \cdot a^{1/2} \quad (2)$$

where c is the trace length of the crack measured from the center of the indentation, a is one half of the average length of the two indent diagonals, and H_v is the hardness.

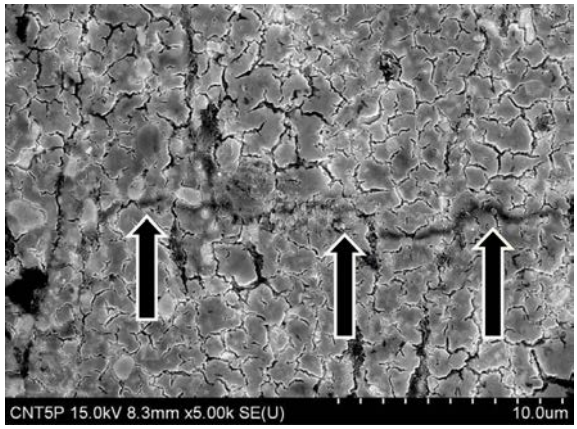

Fig. 8. Median crack propagating of the (W,Ti)C-5 vol.%CNT sintered from powder milled for 10 h.

Hardness of (W,Ti)C, (W,Ti)C-5 vol.% CNT and (W,Ti)C-10 vol.% CNT samples with ball milling for 10 h was 2760, 1870, and 1350 $kg \cdot mm^{-2}$, and their fracture toughness was 7, and 13 $MPa \cdot m^{1/2}$, respectively. These values represent the average of five measurements. In case of (W,Ti)C-10 vol.% CNT sample, fracture toughness can not be calculated because crack was not produced at the indentation corner. A higher magnification view of the indentation median crack in a (W,Ti)C-5 vol.% CNT sample is shown in Fig. 8, which shows that the crack propagated in a deflective manner (↑). The addition of CNT to (W,Ti)C significantly improved the fracture toughness. The enhanced fracture toughness of (W,Ti)C-CNT composite is believed that CNT in the composite may deter the propagation of cracks.

Summary

Nanopowder of (W,Ti)C was fabricated by high energy ball milling. Using the rapid sintering method, PCAS, the densification of (W,Ti)C, (W,Ti)C-5 vol.% CNT and (W,Ti)C-10 vol.% CNT was accomplished using high energy ball milling. The consolidation temperature decreased with addition of CNT. The average grain sizes of the (W,Ti)C in 0 vol.% CNT, 5 vol.% CNT and 10 vol.% CNT calculated from the XRD data were about 60, 52, and 66 nm and their corresponding densities were approximately 99%, respectively. The Vickers Hardness of (W,Ti)C, and (W,Ti)C-5 vol.% CNT samples with ball milling for 10 h was 2760, and 1870 $kg \cdot mm^{-2}$, and their fracture toughness was 7, and 13 $MPa \cdot m^{1/2}$, respectively. The enhanced fracture toughness of (W,Ti)C-CNT composite is believed that CNT in the composite may deter the propagation of cracks

Acknowledgments

This study was supported by a grant in aid awarded by the Basic Research Project of the Korea Institute of Geoscience and Mineral Resources (KIGAM), funded by the Ministry of Science, ICT and Future Planning (GP2015036) and this work was supported by the Human Resources Development program (No.20134030200330) of the Korea Institute of Energy Technology Evaluation and Planning (KETEP) grant funded by the Korea government Ministry of Trade, Industry and Energy.

References

1. S. Imasato, K. Tokumoto, T. Kitada, S. Sakaguchi, Int. J. of Refract. Met. and Hard Mater. 13[5] (1995) 305-312.
2. E.A. Almond, B. Roebuck, Mater. Sci. Eng. A 105/106 (1988) 237-248.
3. G. Gille, J. Bredthauer, B. Gries, B. Mende, Int. J. of Refract. Met. and Hard Mater. 18[2-3] (2000) 87-102.
4. P. Goeuriot, F. Thevenot, Ceramics International 13[2] (1987) 99-103.
5. E.T. Thostenson, Composites Science and Technology 65 (2005) 491-496.
6. L. Fu, LH. Cao, Fan YS, Scripta Materialia 44 (2001) 1061-1065.
7. H.S. Kang, S.J. Lee and I.J. Shon, Journal of Ceramic Processing Research 15[5] (2014) 286-289.
8. S. Berger, R. Porat, R. Rosen, Progress in Materials 42 (1997) 311-322.
9. Z. Fang, JW. Eason, Int. J. of Refractory Met. & Hard Mater. 13 (1995) 297-302.
10. H.S. Kang and I.J. Shon, Korean J. Met. Mater. 52[8] (2014) 623-629.
11. H.S. Kang, J.M. Doh, J.K. Yoon, and I.J. Shon, Korean J. Met. Mater. 52 [10] (2014) 759-764.
12. M. Sommer, W.D. Schubert, E. Zobetz, P. Warbichler, Int. J. of Refractory Met. & Hard Mater. 20 (2002) 41-46.
13. B.R. Kang and I.J. Shon, Korean J. Met. Mater. 53[4] (2015) 255-260.
14. I.J. Shon, H.G. Jo, and H. Kwon, Korean J. Met. Mater. 52[5] (2014) 343-346.
15. I.J. Shon, Korean J. Met. Mater. 52[8] (2014) 573-580.
16. C. Suryanarayana, M.G. Norton, X-ray Diffraction A Practical Approach, Plenum Press, New York, (1998).
17. S.I. Cha and S.H. Hong, Mater. Sci. Eng. A 356 (2003) 381-389.
18. J. Zhao, T. Holland, C. Unuvar and Z.A. Munir, Int. Journal of Refractory Metals & Hard Materials 27 (2009) 130-139.
19. C. Suryanarayana, Prog. Mater. Sci. 46 (2001) 1-184.
20. Z. Shen, M. Johnsson, Z. Zhao and M. Nygren, J. Am. Ceram. Soc. 85, (2002) 1921-1927.
21. J.E. Garay, U. Anselmi-Tamburini, Z.A. Munir, S. C. Glade and P. Asoka- Kumar, Appl. Phys. Lett. 85 (2004) 573-577
22. J.R. Friedman, J.E. Garay. U. Anselmi-Tamburini and Z.A. Munir, Intermetallics 12 (2004) 589-596.
23. J.E. Garay, J.E. Garay. U. Anselmi-Tamburini and Z.A. Munir, Acta Mater. 51 (2003) 4487-4493.
24. K. Niihara, R. Morena, and D.P.H. Hasselman, J. Mater. Sci. Lett. 1 (1982) 12-16.